HOKKAIDO UNIVERSITY

Title	Gene cloning and characterization of a vanadium-dependent bromoperoxidase from the red alga Laurencia saitoi, a producer of brominated diterpenoids and triterpenoids
Author(s)	Kaneko, Kensuke; Kobayashi, Daiki; Masaki, Shiro et al.
Citation	Journal of Applied Phycology, 35, 1443-1452 https://doi.org/10.1007/s10811-023-02953-w
Issue Date	2023-04-10
Doc URL	https://hdl.handle.net/2115/91590
Rights	This version of the article has been accepted for publication, after peer review (when applicable) and is subject to Springer Nature's AM terms of use, but is not the Version of Record and does not reflect post-acceptance improvements, or any corrections. The Version of Record is available online at: http://dx.doi.org/10.1007/s10811-023-02953-w
Type	journal article
File Information	Gene cloning and characterization of a vanadium-dependent bromoperoxidase from the red alga Laurencia saitoi.pdf

Hokkaido University Collection of Scholarly and Academic Papers : HUSCAP

Gene cloning and characterization of a vanadium-dependent bromoperoxidase from the red alga *Laurencia saitoi*, a producer of brominated diterpenoids and triterpenoids

Kensuke Kaneko[1,2]*, Daiki Kobayashi[1], Shiro Masaki[1], Kenji Washio[1,3], Masaaki Morikawa[1,3], and Tatsufumi Okino[1,3,]*

[1] *Graduate School of Environmental Earth Science, Hokkaido University, Sapporo 060-0810, Japan*
[2] *Hachinohe College of Technology, Aomori 039-1192, Japan*
[3] *Faculty of Environmental Earth Science, Hokkaido University, Sapporo 060-0810, Japan*

* Corresponding Authors

Email: kaneko.kensuke.6a@kyoto-u.jp for KK, okino@ees.hokudai.ac.jp for TO

Telephone: +81-178-27-7289 for KK, +81-11-706-4519 for TO

Abstract

The gene encoding vanadium-dependent bromoperoxidase (V-BPO) was cloned for the first time from the red alga *Laurencia saitoi*, which produces pharmaceutically promising brominated diterpenoids and triterpenoids. The molecular weight of V-BPO from *L. saitoi* (*Ls*VBPO1) was the highest (77.0 kDa) among previously reported V-BPOs from *Laurencia* with a peptide insertion Asn194-Ser221 containing short Gln repeats. It shares approximately 60% amino acid sequence identity with V-BPOs from *L. nipponica* (*Ln*VBPO1 and *Ln*VBPO2) and *L. okamurae* (*Lo*VBPO1a and *Lo*VBPO2a). Heterologously expressed *Ls*VBPO1 in *Escherichia coli* was partially purified and exhibited low but significant bromination activity of 38 U mg^{-1} protein using monochlorodimedone. The pH optimum was 8.0, which was more alkaline than that for *Ln*VBPOs and *Lo*VBPO2a (pH 7.0). The K_m for H_2O_2 was 0.04 mM, comparable to *Ln*VBPO1 (0.026 mM), *Ln*VBPO2 (0.025 mM), and *Lo*VBPO2a (0.014 mM). *Ls*VPBO1 retained its bromination activity until 45°C for 20 min. When incubated at 55°C for 20 min, catalytic activity decreased rapidly, as shown for *Ln*VBPO1 and *Lo*VBPO2a (retained

at 45°C, decreased at 55°C) and *Ln*VBPO2 (retained at 55°C, decreased at 65°C). Unlike other V-BPOs from *Laurencia* (*Ln*VBPO1, *Ln*VBPO2, and *Lo*VBPO2a), dialysis and concentration during purification process were rapidly inactivated *Ls*VBPO1, suggesting its structural instability.

Keywords: *Laurencia saitoi*; vanadium-dependent bromoperoxidase (V-BPO); bromination activity; red algae.

1. Introduction

Members of the red algae genus *Laurencia* (Rhodomelaceae, Ceramiales) produce various halogenated (mostly brominated) compounds. The structures of > 700 halogenated compounds were presented in a review by Harizani et al. (2016). These halogenated compounds are categorized by their biosynthetic aspects, such as the non-terpenoids of C_{15} acetogenins, sesquiterpenoids, diterpenoids, triterpenoids, and indoles (Suzuki and Vairappan 2005; Wang et al. 2013; Harizani et al. 2016). Of these, brominated triterpenoids such as thyrsiferol and its derivatives are promising for pharmaceutical applications because of their high cytotoxicity against mouse lymphoid tumor cell line P388 cells (ED_{50} 0.47-17 nM) (Fernández et al. 2000). Because of their strong cytotoxicities, unique structures, and partial enantiodivergency (Hoshino et al. 2017), the biosynthetic mechanisms of brominated triterpenoids are an attractive challenge.

In the view of the field of organic chemistry, a key step in the biosynthesis of brominated triterpenoids is presumed to be the successive poly-etherification of a putative precursor of squalene-tetra/pentaepoxide, triggered by electrophilic attack of Br^+ generated by bromoperoxidase (Hashimoto et al. 1990; Suzuki et al. 1993; Carter-Franklin and Butler 2004; Hoshino et al. 2017). The catalytic assumption of bromonium ion-assisted etherification by bromoperoxidases focuses attention not only on biosynthetic aspects, but also with a view to

organic synthesis (Butler and Sandy 2009; Agarwal et al. 2017; Latham et al. 2018; Höfler et al. 2019). Representative bromoperoxidases in algae are known to coordinate vanadate as a cofactor and the so-called vanadium-dependent bromoperoxidases (V-BPOs) (Wever et al. 2018). However, bromoperoxidases from *Laurencia* producing brominated triterpenoids have not yet been cloned and characterized. On the other hand, in our previous report, V-BPOs from the non-terpenoid of the C_{15} acetogenin producer of *Laurencia nipponica* (*Ln*VBPO1 and *Ln*VBPO2) and the sesquiterpenoid producer of *Laurencia okamurae* (*Lo*VBPO2a) were characterized using a heterologous expression system in *Escherichia coli* (Kaneko et al. 2014; Ishikawa et al. 2022).

To shed light on the biosynthesis of cytotoxic and unique polyetherified structures of brominated triterpenoids, gene cloning and characterization of V-BPO from *L. saitoi* were conducted.

2. Experimental Section

2.1. Plant materials

Laurencia saitoi was collected from Oshoro Bay, Hokkaido, Japan in July 2011 and 2014 (Fig. 1). The collected algae were then transported to a laboratory on ice. The specimens were identified by Dr. Tsuyoshi Abe (Hokkaido University Museum, Hokkaido University, Japan). For LC/MS component analysis, algae were dried at 25-27°C for 1 week and stored at -30°C until use. For *V-BPO* gene cloning, algae were washed with filtered and autoclaved seawater and stored at -80˚C until use.

2.2. LC/MS componential analysis

L. saitoi algal bodies (dry weight 1 g, $n = 3$) were extracted with MeOH. MeOH extracts were dried *in vacuo* and separated using ethyl acetate and water. The ethyl acetate layer was dehydrated using anhydrous Na_2SO_4 and then dried again. Dried samples were dissolved in

MeOH and desalted using Strata C18-E columns (Phenomenex, Torrance, CA, USA). The desalted extracts were subjected to LC/MS analysis at a concentration of 1 mg mL^{-1} in MeOH. Mass spectra were obtained using Accela-LC and LTQ Orbitrap Discovery platforms (Thermo Fisher Scientific, Waltham, MA, USA) in the FT-ESI positive mode. YMC Pack Pro C18 (2.0 × 150 mm) (YMC, Kyoto, Japan) was selected as the analytical column. The elution program was set to a linear gradient of 50-100% MeCN in water containing 0.1% HCOOH (0-20 min), followed by an isocratic gradient of 100% MeCN containing 0.1% HCOOH (20-40 min) at a flow rate of 0.2 mL min^{-1}.

2.3. Partial cloning of LsVBPO1 *by degenerate PCR*

Genomic DNA was prepared from *L. saitoi* collected in July 2011 using phenol-chloroform extraction and used as a PCR template. Takara Ex Taq (Takara Bio, Shiga, Japan) was used under the following conditions: 94°C for 3 min, 32 cycles of 94°C for 30 s, 52°C for 1 min, and 72°C for 30 s, followed by a final elongation step at 72°C for 3 min. The degenerate primers (pair 1 in Table S1) were designed by referencing a conserved vanadate active center in *V-BPOs* from *L. nipponica* (*Ln*VBPO1 and *Ln*VBPO2, Kaneko et al. 2014) and one from the red algae *Corallina* spp., whose X-ray crystal structures have been solved (Isupov et al. 2000; Littlechild and Garcia-Rodriguez 2003). The amplified DNA was subjected to TBE 1.0% agarose gel electrophoresis. The target band was excised, purified using a Quick Gel Extraction Kit (Qiagen, Venlo, Netherlands), and subcloned into the pGEM-T Easy Vector (Promega, Fitchburg, WI, USA). Plasmids were transformed into *E. coli* DH5α cells and purified using the QIAprep Spin Miniprep Kit (Qiagen) for Sanger DNA sequencing using the BigDye Direct Sequencing Kit on an ABI3130 instrument (Applied Biosystems, Foster City, CA, USA). The partial *V-BPO* sequences obtained were analyzed using NCBI BLAST (https://blast.ncbi.nlm.nih.gov/Blast.cgi) and Genetyx (GENETYX Corporation, Tokyo,

Japan).

2.4. Partial cloning of LsVBPO1 *by inverse PCR*

Three independent inverse PCR amplification were conducted (Scheme S1). First, genomic DNA from *L. saitoi* was digested with *Xho*I (Takara Bio, Shiga, Japan). The digested genome was self-ligated using the Takara DNA Ligation Kit Ver 1 (Takara Bio) and used as the PCR template. Primers were designed by referencing the partial *V-BPO* sequence obtained from the degenerate PCR in ***2.3*** (pair 2 in Table S1). Takara Ex Taq was used under the following conditions: 94°C for 3 min, 33 cycles of 94°C for 1 min, 55°C for 1 min, and 72°C for 2 min, followed by a final elongation step at 72°C for 5 min. The amplified PCR products were subjected to nested PCR using primer pair 3 (Table S1) under the same conditions. Amplicons were checked using TBE 1.0% agarose gel electrophoresis for sequencing. Partial sequences of *V-BPO* spanning 1-474 bp and 1,044-1,488 bp were obtained (Fig. S2). Second, the genomic DNA was digested with *Nsi*I (Takara Bio) and self-ligated to the PCR template. The PCR experiments were conducted under the same conditions as described above. The primer pairs used were pair 4 in the 1st round and pair 5 in the 2nd round (Table S1). *V-BPO* partial sequences ranging from 1,482 bp to 1,742 bp were acquired (Fig. S2). Finally, the genomic DNA was digested with *Aat*II (Takara Bio) and self-ligated to the PCR template. Takara LA Taq (Takara Bio) was used for the 1st and 2nd rounds of PCR under the following conditions: 94°C for 3 min, 33 cycles at 94°C for 1 min, 55°C for 1 min, and 72°C for 2 min, followed by a final elongation at 72°C for 5 min. The primer pairs used were pair 6 in the 1st round and pair 7 in the 2nd round (Table S1). A partial sequence of *V-BPO* from 1,693 bp to the stop codon at 2,109 bp was obtained (Fig. S2).

2.5. Full length cloning of LsVBPO1

Degenerate PCR (***2.3.***) and inverse PCR (***2.4.***) provided five cumulative partial sequences of *V-BPO* coding from the first Met to the stop codon (Scheme S1). Next, a primer pair amplifying full-length *V-BPO* was designed (pair 8 in Table S1). A full-length sequence of *V-BPO* was amplified using KOD Dash (Toyobo, Osaka, Japan) under the following conditions: 94°C for 2 min, 25 cycles at 94°C for 30 s, 56°C for 5 s, and 74˚C for 1.5 min. After ethanol precipitation, the amplified PCR products were digested with *Nde*I and *Bam*HI (Takara Bio) to generate pET21a (Merck, Darmstadt, Germany). pET21a was introduced using the Takara DNA Ligation Kit v.1 (Takara Bio). The pET21a vector carrying the full-length *V-BPO* coding sequence, including the stop codon, was transformed into Nova Blue *E. coli* cells (Merck) for DNA sequencing. After verifying the correct sequence and insertion, the sequence was deposited with DDBJ (https://www.ddbj.nig.ac.jp/index.html) as *V-BPO* from *L. saitoi*, *LsVBPO1* (accession No. LC730855). Alignment and phylogenetic analyses were performed using BioEdit (Hall 1999) and MEGA X (Kumar et al. 2018). The structural prediction model of *Ls*VBPO1 was calculated using SWISS-MODEL (https://swissmodel.expasy.org/) and visualized by PyMOL (https://pymol.org/2/). For the modeling, the X-ray crystal structure of V-BPO from the red alga *Corallina pilulifera* at 2.20 Å (1up8.1.A in PDB) was chosen as template.

2.6. Amplification of LsVBPO1 *from cDNA*

L. saitoi collected at Oshoro Bay in July 2011 and 2014 were subjected to total RNA preparation using the RNeasy Midi kit (Qiagen). After digestion of genomic DNA and purification of poly $(A)^+$ RNA using the Oligotex^{TM}-dT30 <Super> mRNA purification kit (Takara Bio), cDNA was prepared using the Marathon cDNA Amplification Kit (Takara Bio). PCR amplification was performed using Takara Ex Taq and primer pair 8 (Table S1) under the following conditions:94°C for 3 min, 32 cycles of 94°C for 1 min, 48°C for 1 min, and 72°C

for 2 min, followed by a final elongation step at 72°C for 3 min. The amplified products were analyzed using TBE 1.0% agarose gel electrophoresis.

2.7. Construction and purification of recombinant Ls*VBPO1 protein*

pET21a vector carrying full-length *LsVBPO1* (***2.5.***) was electroporated into *E. coli* expression cells strain BL21 (DE3) pLys (Takara Bio) for purification of the recombinant protein without a tag. Purification was conducted according to the previously characterized *Ln*VBPO1 and *Ln*VBPO2 (Kaneko et al. 2014). The *E. coli* strain carrying *LsVBPO1* constructed above was cultured in 1 L LB medium containing 50 μg mL^{-1} carbenicillin disodium salt at 37°C with rotary agitation (120 rpm min^{-1}) until the mid-log phase. The expression of *LsVBPO1* was induced by 0.4 mM isopropyl-β-D-thiogalactopyranoside (IPTG) at 25°C. The induced *Ls*VBPO1 protein was harvested as the soluble fraction using 50 mM Tris-H_2SO_4 (pH 8.0) buffer containing 1 mM NH_4VO_3. The soluble fraction was subjected to 30% saturation with ammonium sulfate and precipitation. The supernatant was subjected to DE52 anion exchange chromatography (GE Healthcare, Buckinghamshire, UK) using stepwise elution with KBr (0.1, 0.2, 0.3, 0.4, and 0.8 M) in 50 mM Tris-H_2SO_4 (pH 8.0) buffer containing 1 mM NH_4VO_3. The fraction containing *Ls*VBPO1 was guided by 10% SDS-PAGE (Laemmli 1970) using CBB and in-gel active staining with *o*-dianisidine; reaction mixture of 1 mM *o*-dianisidine (Tokyo Kasei, Tokyo, Japan), 0.1 mM NH_4VO_3, 100 mM KBr, 100 mM sodium phosphate buffer (pH 6.5) and 2 mM H_2O_2 (Carter et al. 2002). Protein concentrations of the eluents were quantified using a BCA protein assay kit (Thermo Scientific, Waltham, MA, USA).

2.8. Verification of bromination activity of Ls*VBPO1*

Bromination activity of the recombinant *Ls*VBPO1 protein was assayed spectrophotometrically at 25°C by measuring the decrease in optical absorbance at 290 nm

upon bromination of monochlorodimedone (MCD, $\varepsilon = 19.9\ mM^{-1}\ cm^{-1}$, pH 6.0) to monobromo-monochlorodimedone. The standard conditions were 50 mM MES-NaOH (pH 6.0), 200 mM KBr, 50 μM MCD, and 1 mM H_2O_2 (Bernhardt et al. 2011; Kaneko et al. 2014). One unit (U) was defined as the conversion of 1 μmol of MCD per min. MCD was purchased from Alfa Aesar (Ward Hill, MA, USA). The pH dependence was tested between pH 4.0 and 10.0. Two buffer systems were used: 50 mM MES-NaOH at pH 4.0-7.0 and 50 mM Tris-HCl at pH 8.0-10.0. To retain the ionic strength in different buffer systems, 0.15 M Na_2SO_4 was added (Wever et al. 2018). Thermal stability was analyzed using standard assay conditions after treatment of the enzymes at various temperatures (25‑85°C) for 20 min. Steady-state kinetic experiments were performed by varying the concentration of one of the substrates (0.01, 0.03, 0.06, 0.1, 0.15 and 0.2 mM H_2O_2 or 0.1, 0.25, 0.5, 1.0, 2.5, and 5.0 mM KBr) while fixing the concentration of the second substrate at a saturating concentration (200 mM KBr to determine the K_m for H_2O_2, 1 mM H_2O_2 to determine the K_m for Br^-). Kinetic experiments were performed at pH 6.0, to compare the K_m values of other red algae, including *L. nipponica* and *L. okamurae*. K_m values were derived from non-linear fitting of the initial rate data using GraphPad Prism (GraphPad Software, San Diego, CA, USA). Chlorination activity was tested by adding 0.2 or 1.5 M KCl instead of 0.2 M KBr under the standard conditions (Soedjak and Butler 1990; Rush et al. 1995; Ohshiro et al. 2002). All experiments were performed in triplicate.

3. Results

3.1. LC/MS componential analysis of L. saitoi

The red algal genus *Laurencia* produces various brominated compounds. These brominated compounds are classified based on their biosynthetic background: C_{15} acetogenins, sesquiterpenoids, diterpenoids, triterpenoids, and indoles. According to a comprehensive review of *Laurencia* brominated compounds in Japanese coastal areas, *L. saitoi* in Oshoro Bay

is known to produce brominated diterpenoids and triterpenoids, such as parguerols and thyrsiferols (Suzuki and Vairappan 2005). Our LC/MS componential analysis of *L. saitoi* showed ions corresponding to the *m/z* of brominated diterpenoid parguerol as well as brominated triterpenoids of thyrsiferols and magireol A. However, ions corresponding to other brominated compounds (*e.g.*, C_{15} acetogenins) appeared to be absent (Fig. S1). Thus, gene cloning of *V-BPO* from *L. saitoi* was performed as a producer of brominated diterpenoids and triterpenoids.

3.2. Gene cloning of LsVBPO1

L. saitoi in Oshoro Bay grows seasonally during July. If the expression of *V-BPO*(s) in *L. saitoi* was transient, cloning from cDNA might have overlooked it. To ensure cloning, genomic DNA was first used. Genomic DNA from *Laurencia saitoi* collected in Oshoro Bay in July 2011 (Fig. 1) was subjected to degenerate PCR. A partial sequence of *V-BPO* was successfully obtained (489-1,074 bp; Fig. S2). By repeating the inverse PCR experiments (Scheme S1), four additional partial sequences of *V-BPO* covering the first Met to the stop codon were acquired (1-474, 1,044-1,488, 1,482-1,742, and 1,693-2,109 bp in Fig. S2). By referencing these five partial sequences, primer pair 8 (Table S1) was designed to amplify full-length *V-BPO* from *L. saitoi* genomic DNA. The full-length sequence was intron-less (2,109 bp, encoding 702 deduced amino acids; Fig. S2), which coincides with the features of red algal genomes (Collén et al. 2013). Amino acid residues comprising the active center of V-BPO that coordinate vanadate cofactors are well-conserved (Messerschmidt and Wever 1996; Weyand et al. 1999; Isupov et al. 2000; Littlechild and Garcia-Rodriguez 2003; McLauchlan et al. 2019). The deduced amino acid sequence of cloned *V-BPO* shares ~60% identity with previously characterized *Laurencia* V-BPOs; *Ln*VBPO1 and *Ln*VBPO2 from *L. nipponica* share 95% amino acid identity (Kaneko et al. 2014), *Lo*VBPO1s and *Lo*VBPO2s from *L. okamurae* share 98% amino acid identity (Ishikawa et al. 2022). A remarkable feature of *Ln*VBPOs and

*Lo*VBPO2a, an insertion containing Gln repeats (Gly512-Thr568), was also confirmed. A short insert ranging from Asn194-Ser221 containing Gln repeats was specific to cloned V-BPO (Fig. 2). Phylogenetic tree analysis showed that the cloned V-BPO branched into the clade of V-BPOs from *Laurencia* (Fig. S3). We named the *V-BPO* cloned from *L. saitoi LsVBPO1*.

3.3. Comparison of **LsVBPO1** *from genomic DNA and cDNA*

LsVBPO1 was amplified from the cDNA of *L. saitoi* to compare *LsVBPO1* cloned from genomic DNA. As the bloom of *L. saitoi* in Oshoro Bay is transient in July, cDNA was prepared from *L. saitoi* collected in July 2011 and 2014. All PCR products derived from cDNA using primer pair 8 (Table S1) exhibited bands around 2.0 kb, the same mobility as the PCR product from genomic DNA (Fig. S4).

3.4. Preparation of recombinant **Ls*VBPO1* protein**

Recombinant *Ls*VBPO1 protein without a tag was prepared using an *E. coli* expression system according to *Ln*VBPO1 and *Ln*VBPO2 from *L. nipponica* (Kaneko et al. 2014). The IPTG-induced recombinant protein of *Ls*VBPO1 was eluted in 0.8 M KBr fraction of DE52 anion-exchange chromatography, which was confirmed by 10% SDS-PAGE with CBB and *o*-dianisidine staining (Fig. 3). However, in contrast to the recombinant proteins of *Ln*VBPOs and *Lo*VBPO2a, *Ls*VBPO1 eluted in the 0.8 M KBr fraction was still not pure. Dialysis or concentration, as in *Ln*VBPOs (Kaneko et al. 2014) and *Lo*VBPO2a (Ishikawa et al. 2022) for further purification, failed to retain its activity. Therefore, we utilized the 0.8 M KBr fraction as partially purified *Ls*VBPO1, with a total protein concentration of 29 μg mL^{-1} (as calculated by the BCA method), for further characterization.

3.5. Bromination activity of recombinant **Ls*VBPO1* protein**

According to the MCD assay under standard conditions, bromination activity was estimated

to be 38 U mg^{-1} protein. The addition of vanadate ($NaVO_3$) enhanced the bromination activity ($P < 0.05$, Student's *t*-test, Fig. S5). The optimum pH was 8.0, and activity was nearly disappeared at pH 4.0 (Fig. 4a). The activity rapidly decreased after incubation at 55°C for 20 min (23% compared to that at 25°C, Fig. 4b). It was not possible to recover the activity of *Ls*VBPO1 that was inactivated by heat treatment at 75°C for 20 min, by incubating the enzyme at 4°C for 20 min. The K_m and V_{max} values for H_2O_2 were determined as 0.04 (± 0.00, standard deviation) mM and 76.1 (± 2.7, standard deviation) U mg^{-1} protein, respectively (Fig. 5). However, K_m and V_{max} for Br^- were not calculated (Fig. S6). MCD-chlorination activity was not detected at concentrations of 0.2 and 1.5 M KCl.

4. Discussion

LsVBPO1 was cloned from *L. saitoi*, a producer of various brominated triterpenoids and diterpenoids (Suzuki et al. 1985; Kurata et al. 1998; Suzuki and Vairappan 2005). In another genus of *Laurencia*, we cloned *LnVBPOs* from *L. nipponica* producing brominated C_{15} acetogenin of laurencin (Kaneko et al. 2014), and *LoVBPOs* from *L. okamurae* produces brominated sesquiterpenoids (Ishikawa et al. 2022). Despite difference in the carbon skeletons of the putative precursors, the biosynthesis of brominated triterpenoids, C_{15} acetogenins, and sesquiterpenoids are considered to initiate an electrophilic attack of Br^+ (Fukuzawa et al 1994; Carter-Franklin and Butler 2004; Bonney and Braddock 2012; Taylor and Fox 2015; Hoshino et al. 2017; Zhang et al. 2019; Chan et al. 2019). Therefore, characterization and comparison of V-BPOs from *Laurencia*, an enzyme that oxidizes bromide to bromonium ions, is crucial. A comparison of the biochemical behaviors of V-BPOs in *Laurencia* (*L. saitoi*, *L. nipponica*, and *L. okamurae*) is summarized in Table 1.

*Ls*VBPO1 shares approximately 60% amino acid identity with previously characterized V-BPOs from *L. nipponica* and *L. okamurae* (Kaneko et al. 2014; Ishikawa et al. 2022). These

Laurencia-derived V-BPOs contain a remarkable insertion consisting of Gln repeats (Gly512-Thr568 in Fig. 2). Since this insertion is not found in other algal V-BPOs, it might be a characteristic feature of *Laurencia*. In *Ls*VBPO1, an additional short insert is found at Asn194-Ser221 with short Gln repeats (Fig. 2, Table 1). Although the structural and physiological roles remain uncertain, Gln repeats might affect the folding and biochemical behavior of V-BPOs from *Laurencia* (Ishikawa et al. 2022). In contrast to cDNA-cloned *LnVBPOs*, *LsVBPO1* was isolated from genomic DNA without introns. PCR amplicons from cDNA using the same primer pair showed bands at 2.0 kb as shown for the amplicon from genomic DNA (Fig. S4).

E. coli-expressed recombinant *Ls*VBPO1 was eluted in a 0.8 M KBr fraction, as was the case for *Ln*VBPO2 and *Lo*VBPO2a (Kaneko et al. 2014; Ishikawa et al. 2022). However, unlike *Ln*VBPOs and *Lo*VBPO2a, the eluent contained only partially purified enzyme (Fig. 3). Because the same *E. coli* host and purification procedures were utilized, some amino acid residues specific for *Ls*VBPO1 (*e.g.*, insertion at Asn194-Ser221) might cause unusual protein folding or aggregation with *E. coli* proteins during purification.

In the prediction model of V-BPOs from *Laurencia* (*Ln*VBPO1, *Ln*VBPO2, *Lo*VBPO2a, and *Ls*VBPO1), Gln repeats feature in *Laurencia* (Gly512-Thr568) were visualized as huge outstanding loops to make rather bulky forms compared to X-ray crystal structure of *Corallina* V-BPO (Fig. S7). Red algal V-BPOs form homo-dimer based dodecamer by hydrogen bonds. This multimeric structure with hydrogen bonds considered to link with thermostability of V-BPO enzyme (Isupov et al. 2000; Ohshiro et al. 2002; Littlechild and Garcia-Rodriguez 2003). Since the recombinant proteins of *Corallina* V-BPOs tend to show high thermostability (> 80°C) than *Ln*VBPOs and *Lo*VBPO2a (Ohshiro et al. 2002; Kaneko et al. 2014; Ishikawa et al. 2022), these outstanding Gln loops (Gly512-Thr568) may impair the compact multimeric forms like *Corallina* V-BPOs. According to a superimpose analysis with *C. pilulifera* V-BPO, another short insert containing Gln repeats, specific for *Ls*VBPO1 (Asn194-Ser221) was also

predicted as outstanding loop (Fig. S8). Therefore, *Ls*VBPO1 might be the most bulk structure in *Laurencia* V-BPOs.

In mammals, such unusual poly Gln expansions trigger protein misfolding and aggregation and eventually cause neuro-diseases, such as polyglutamine diseases of Huntingtin disease (Fujino and Nagai 2022). Gln repeats are also identified in various plant proteins. In *Arabidopsis thaliana*, early flowering 3 protein (ELF3) contains Gln repeats. ELF3 is a "hub protein" to interact various proteins and play a core component of the circadian clock and a potent repressor of flowering. The Gln repeats in a hub-protein of ELF3 is considered to drive adaptation to internal genetic environments (Undurraga et al. 2012). In *Populus trichocarpa*, a C-terminus binding protein ANGUSTIFOLIA contains a Gln repeats. Although their physiological functions remain unknown, protein variants consisting of the different number of Glns (Gln 11, 13, and 15 repeats) are found and show the different cellular localizations. The Gln 11 and Gln 15 variants located at nuclear and cytosol, respectively, while the Gln 13 variant localized in both (Bryan et al. 2018). These imply that the Gln repeats causing aggregation in mammalian cells might not be unsuitable and might have some physiological roles in plants. Indeed, the different aggregation effects of Gln repeats in mammalian and plant cells are discussed by overexpression of an aggregation-prone fragment of human Huntingtin protein (HTT) containing Gln 69 repeats in plant cells *A. thaliana*. Interestingly, while the HTT caused aggregation in invertebrate and mammalian transgenic models, aggregation was suppressed in plant cells (Llamas et al. 2022).

Structural tendency and physiological rolls of Gln repeats for *Ls*VBPO1 (Asn194-Ser221 and Gly512-Thr568) are unknown. However, as instances in ELF3, ANGUSTIFOLIA, and overexpression of HTT in plant cells, Gln repeats in *Ls*VBPO1 might have some physiological rolls to adapt the enzyme to environment and location in *L. saitoi* alga. *Laurencia* produces various brominated compounds and stores them in the specific storage organelle *corps en cerise*

(Fig. 1). The Gln repeats in *Ls*VBPO1 and V-BPOs from *Laurencia* might regulate cellular location to simplify the transport and storage of brominated compounds which they may produce into the organelle *corps en cerise*.

Partially purified *Ls*VBPO1 (0.8 M KBr) was directly used to evaluate biochemical behavior. MCD-bromination activity was 38 U mg^{-1} protein, which was significantly lower than that of purified recombinant *Ln*VBPO1 (443 U mg^{-1} protein), *Ln*VBPO2 (434 U mg^{-1} protein), and *Lo*VBPO2a (477 U mg^{-1} protein). In contrast, *Ls*VBPO1 showed similar thermostability to that of *L. nipponica* and *L. okamurae* (Table 1). Unlike other V-BPOs that can reform hydrogen bonds for active homodimer-based dodecameric multimerization in the red algae *Corallina* species (Isupov et al. 2000; Ohshiro et al. 2002; Littlechild and Garcia-Rodriguez 2003) and the cyanobacterium *Acaryochloris marina* which also contains *inter*-/*intra*- disulfide bonds (Frank et al. 2016), cooling heat-treated *Ls*VBPO1 at 4°C did not recover activity. This implied not only low purity but also labile protein structure, which might impair the reconstruction of hydrogen bonds for multimerization.

The optimum pH of *Ls*VBPO1 was speculated to be an alkaline pH of 8.0, which is comparable to that of seawater (pH 8.1). In other *Laurencia* V-BPOs, *Ln*VBPOs and *Lo*VBPO2a were neutral at pH 7.0 (Table 1). Generally, most native or recombinant red algal V-BPOs showed an acidic optimum pH of 6.0 or neutral pH (7.0). The relationship between the habitat and optimum pH of red algal V-BPOs has been reported (Baharum et al. 2013). V-BPOs showing an optimum pH of 6.0 or 7.0 are from the algae in the intertidal zone. The habitat of *L. saitoi* in Oshoro Bay, which was sampled, is 2.0-3.0 m deep in a subtidal zone. On the other hand, the habitats of *L. nipponica* and *L. okamurae* in Oshoro-Bay were 0.3-1.0 m deep in an intertidal zone. These differences in and preferences of *L. saitoi* may contribute to the optimal pH of V-BPOs.

*Ls*VBPO1 exhibited high affinity for H_2O_2 with a K_m value of 0.04 mM, similar to those of

*Ln*VBPO1 (0.026 mM), *Ln*VBPO2 (0.025 mM), and *Lo*VBPO2a (0.014 mM) (Table 1). In the paradigm of the other red algal V-BPOs, the purified native and recombinant proteins of *Corallina pilulifera* are 0.092 mM (Ito et al. 1986) and 0.1 mM (Ohshiro et al. 2004) respectively. In *C. officinalis*, 0.06 mM is reported for native V-BPO (Sheffield et al. 1993), and 0.017 mM for a recombinant one (Carter et al 2002). The brown algal V-BPO from *Ascophyllum nodosum* and the cyanobacterial V-BPO from *Acaryochloris marina* also show similar K_m values; 0.055 and 0.06 mM, respectively (Wischang and Hartung 2011; Frank et al. 2016). The generation of H_2O_2 during photosynthesis and photorespiration has harmful effects on algal physiology (Mata et al. 2010; Wever and van der Horst 2013). The low K_m value of *Ls*VBPO1, despite its low purity, supports the role of V-BPO against oxidative stresses in various algae (Wever et al. 2018). The K_m for Br^- was not calculated. The eluent of the 0.8 M KBr fraction was directly used without dialysis, exchanging Br^--free buffer to avoid inactivation. Endogenous Br^- might interfere with the visualization of dose-dependent effects. These results suggested that *Ls*VBPO1 is less stable than *Ln*VBPO1 or *Ln*VBPO2. Currently, it is unknown whether the labile nature of *Ls*VBPO1 is due to the purification process of the recombinant system. Further efforts to overcome its labile features, as well as new attempts, such as quasi-real-time bromination reaction monitoring using online coupling of digital microfluidics and mass spectrometry (Das et al. 2022), might shed light on the enzymatic nature of *Ls*VBPO1.

The structural diversity of brominated compounds in *Laurencia* is an attractive but challenging topic for marine natural products (Harizani et al. 2016). From an organic chemistry viewpoint, Br^+-assisted etherification is assumed to play a key role. Based on this assumption, putative precursors of C_{15} acetogenins, sesquiterpenoids, and triterpenoids are predicted to be laurediol, nerolidol/farnesol, and squalene-tetra/pentaepoxide (Carter-Franklin and Butler 2004; Suzuki and Vairappan 2005; Hashimoto et al. 1990; Hoshino et al. 2017). V-BPO, an

enzyme that catalyzes the oxidation of bromine anions, is considered a strong candidate for the bromination and etherification of these precursors (Butler and Sandy 2009; Agarwal et al. 2017; Latham et al. 2018; Höfler et al. 2019). Nevertheless, recombinant proteins of V-BPOs from *Laurencia* have low *in vitro* bromination efficiency for putative precursors of C_{15} acetogenins (Kaneko et al. 2014) and sesquiterpenoids (Ishikawa et al. 2022). Moreover, *Ls*VBPO1, the first V-BPO obtained from *L. saitoi* exhibited labile features and low bromination activity by MCD. We should take note of the concealed V-BPO(s) and other relevant enzyme(s), as well as different candidate precursors. Meanwhile, a panel of *Laurencia* V-BPOs (*Ls*VBPO1, *Ln*VBPOs, and *Lo*VBPOs) is essential for understanding the biosynthesis and diversity of *Laurencia* brominated compounds.

In conclusion, a novel vanadium-dependent bromoperoxidase (*LsVBPO1*) was cloned from *Laurencia saitoi*. To the best of our knowledge, this is the first report of cloning and evaluation of recombinant V-BPO from a brominated diterpenoid and triterpenoid producer in *Laurencia*. The different biochemical characteristics of the recombinant protein of *Ls*VBPO1 from other *Laurencia* V-BPOs and insertion of additional Gln repeats may be related to the production of different types of brominated compounds.

Author contributions

Kensuke Kaneko conceived and designed experiments, conducted all experiments, and wrote the paper. Daiki Kobayashi, Shiro Masaki, and Kenji Washio cloned and heterologously expressed *Ls*VBPO1. Masaaki Morikawa wrote and revised the manuscript accordingly. Tatsufumi Okino conceived and designed experiments, and wrote the manuscript. All authors have reviewed the manuscript.

Acknowledgments

Kensuke Kaneko thanks the GCOE program of the Graduate School of Environmental Science at Hokkaido University. We thank Prof. Minoru Suzuki and Dr. Tsuyoshi Abe (Hokkaido University) for their valuable advice and suggestions. We are grateful to the staff of the Oshoro Marine Station, Field Science Center for Northern Biosphere, Hokkaido University, for their support and assistance during the field survey. We would like to thank Editage (www.editage.com) for English language editing.

Funding

This work was supported by a JSPS KAKENHI grant (No. 16H04975).

Data availability
The datasets generated and/or analyzed during the current study are available from the corresponding author upon reasonable request.

Competing interests
The authors declare no conflict of interest regarding the publication of this paper.

References
Agarwal V, Miles ZD, Winter JM, Eustáquio AS, El Gamal AA, Moore BS (2017) Enzymatic halogenation and dehalogenation reactions: pervasive and mechanistically diverse. Chem Rev 117:5619-5674.

Baharum H, Chu WC, Teo SS, Ng KY, Abdul Rahim R, Ho CL (2013) Molecular cloning, homology modeling and site-directed mutagenesis of vanadium-dependent bromoperoxidase (GcVBPO1) from *Gracilaria changii* (Rhodophyta). Phytochem 92:49-59.

Bernhardt P, Okino T, Winter JM, Miyanaga A, Moore BS (2011) A stereoselective vanadium-dependent chloroperoxidase in bacterial antibiotic biosynthesis. J Am Chem Soc 133:4268-4270.

Bonney KJ, Braddock DC (2012) A unifying stereochemical analysis for the formation of halogenated C15-acetogenin medium-ring ethers from *Laurencia* species via intramolecular bromonium ion assisted epoxide ring-opening and experimental corroboration with a model epoxide. J Org Chem 77:9574-9584.

Bryan AC, Zhang J, Guo J, Ranjan P, Singan V, Barry K, Schmutz J, Weighill D, Jacobson D, Jawdy S, Tuskan GA, Chen J, Muchero W. (2018). A variable polyglutamine repeat affects subcellular localization and regulatory activity of a *Populus* ANGUSTIFOLIA protein. G3-Genes Genom Genet 8:2631-2641.

Butler A, Sandy M. (2009) Mechanistic considerations of halogenating enzymes. Nature, 460:848-854.

Carter JN, Beatty KE, Simpson MT, Butler A (2002) Reactivity of recombinant and mutant vanadium bromoperoxidase from the red alga *Corallina officinalis*. J Inorg Biochem 91:59-69.

Carter-Franklin JN, Butler A (2004) Vanadium bromoperoxidase-catalyzed biosynthesis of halogenated marine natural products. J Am Chem Soc 126:15060-15066.

Chan HSS, Nguyen QNN, Paton RS, Burton JW (2019). Synthesis, characterization, and reactivity of complex tricyclic oxonium ions, proposed intermediates in natural product biosynthesis. J Am Chem Soc 141:15951−15962.

Collén J, Porcel B, Carré W, Ball SG, Chaparro C, Tonon T, Barbeyron T, Michel G, Noel B, Valentin K, *et al* (2013) Genome structure and metabolic features in the red seaweed *Chondrus crispus* shed light on evolution of the Archaeplastida. Proc Natl Acad Sci 110:5247-5252.

Das A, Weise C, Polack M, Urban RD, Krafft B, Hasan S, Westphal H, Warias R, Schmidt S, Gulder T, Belder D (2022) On-the-fly mass spectrometry in digital microfluidics enabled by a microspray hole: toward multidimensional reaction monitoring in automated synthesis platforms. J Am Chem Soc 144:10353-10360.

Fernández JJ, Souto ML, Norte M (2000) Marine polyether triterpenes. Nat Prod Rep 17:235-246.

Frank A, Seel CJ, Groll M, Gulder T (2016) Characterization of a cyanobacterial haloperoxidase and evaluation of its biocatalytic halogenation potential. ChemBioChem 17:2028-2032.

Fujino Y, Nagai Y (2022) The molecular pathogenesis of repeat expansion diseases. Biochem Soc Trans 50:119-134.

Fukuzawa A, Aye M, Takasugi Y, Nakamura M, Tamura M, Murai A (1994) Enzymatic bromo-ether cyclization of laurediols with bromoperoxidase. Chem Lett 23:2307-2310.

Hall TA (1999) BioEdit: A user-friendly biological sequence alignment editor and analysis program for Windows 95/98/NT. Nucleic Acids Symp Ser 41:95-98.

Harizani M, Ioannou E, Roussis V (2016) The *Laurencia* paradox: an endless source of chemodiversity. Prog Chem Org Nat Prod 102:91-252.

Hashimoto M, Kan T, Nozaki K, Yanagiya M, Shirahama H, Matsumoto T (1990) Total syntheses of (+)-thyrsiferol, (+)-thyrsiferyl 23-acetate, and (+)-venustatriol. J Org Chem 55:5088-5107.

Höfler GT, But A, Hollmann F (2019) Haloperoxidases as catalysts in organic synthesis. Org Biomol Chem 17:9267-9274.

Hoshino A, Nakai H, Morino M, Nishikawa K, Kodama T, Nishikibe K, Morimoto Y (2017) Total synthesis of the cytotoxic marine triterpenoid isodehydrothyrsiferol reveals partial enantiodivergency in the thyrsiferol family of natural products. Angew Chem Int Ed 56:3064-3068.

Ishikawa T, Washio K, Kaneko K, Tang X R, Morikawa M, Okino T (2022) Characterization of vanadium-dependent bromoperoxidases involved in the production of brominated sesquiterpenes by the red alga *Laurencia okamurae*. App Phycol 3:120-131.

Isupov MN, Dalby AR, Brindley AA, Izumi Y, Tanabe T, Murshudov GN, Littlechild JA (2000) Crystal structure of dodecameric vanadium-dependent bromoperoxidase from the red algae *Corallina officinalis*. J Mol Biol 299:1035-1049.

Itoh N, Izumi Y, Yamada H (1986) Characterization of nonheme type bromoperoxidase in *Corallina pilulifera*. J Biol Chem 261:5194-5200.

Kaneko K, Washio K, Umezawa T, Matsuda F, Morikawa M, Okino T (2014) cDNA cloning and characterization of vanadium-dependent bromoperoxidases from the red alga *Laurencia nipponica*. Biosci Biotechnol Biochem 78:1310-1319.

Kumar S, Stecher G, Li M, Knyaz C, Tamura K (2018). MEGA X: Molecular evolutionary genetics analysis across computing platforms. Mol Biol Evol 35:1547-1549.

Kurata K, Taniguchi K, Agatsuma Y, Suzuki M (1998) Diterpenoid feeding-detergents from *Laurencia saitoi*. Phymchem 47:363-369.

Laemmli UK (1970) Cleavage of structural proteins during the assembly of the head of bacteriophage T4. Nature 227:680-685.

Latham J, Brandenburger E, Shepherd SA, Menon BRK, Micklefield J (2018) Development of Halogenase Enzymes for Use in Synthesis. Chem Rev 118:232-269.

Littlechild J, Garcia-Rodriguez E (2003) Structural studies on the dodecameric vanadium bromoperoxidase from *Corallina* species. Coord Chem Rev 237:65-76.

Llamas E, Koyuncu S, Lee HJ, Gutierrez-Garcia R, Dunken N, Charura N, Torres-Montilla S, Schlimgen E, Pulido P, Rodriguez-Concepcion M, Zuccaro A, Vilchez D (2022). Chloroplast protein import determines plant proteostasis and retrograde signaling. bioRxiv preprint https://doi.org/10.1101/2022.03.19.484971.

McLauchlan CC, Murakami HA, Wallace CA, Crans DC (2019). Coordination environment changes of the vanadium in vanadium-dependent haloperoxidase enzymes. J Inorg Biochem 186:267-279.

Mata L, Gaspar H, Justino F, Santos R (2011) Effects of hydrogen peroxide on the content of major volatile halogenated compounds in the red alga *Asparagopsis taxiformis* (Bonnemaisoniaceae). J Appl Phycol 23:827-832

Messerschmidt A, Wever R (1996) X-ray structure of a vanadium-containing enzyme: Chloroperoxidase from the fungus *Curvularia inaequalis*. Proc Natl Acad Sci 93:392-396.

Ohshiro T, Hemrika W, Aibara T, Wever R, Izumi Y (2002) Expression of the vanadium-

dependent bromoperoxidase gene from a marine macro-alga *Corallina pilulifera* in *Saccharomyces cerevisiae* and characterization of the recombinant enzyme. Phytochem 60:595-601.

Ohshiro T, Littlechild J, Garcia-Rodriguez E, Isupov MN, Iida Y, Kobayashi T, Izumi Y (2004) Modification of halogen specificity of a vanadium-dependent bromoperoxidase. Protein Sci 13:1566-1571.

Rush C, Willetts A, Davies G, Dauter Z, Watson H, Littlechild J (1995) Purification, crystallisation and preliminary X-ray analysis of the vanadium-dependent haloperoxidase from *Corallina officinalis*. FEBS Lett 359:244-246.

Sheffield DJ, Harry T, Smith AJ, Rogers LT (1993). Purification and characterization of the vanadium bromoperoxidase from the macroalga *Corallina officinalis*. Phytochem 32:21-26.

Shimonishi M, Kuwamoto S, Inoue H, Wever R, Ohshiro T, Izumi Y, Tanabe T (1998). Cloning and expression of the gene for a vanadium-dependent bromoperoxidase from a marine macro-alga, *Corallina pilulifera*, FEBS Lett 428:105-110.

Soedjak HS, and Butler A (1990) Chlorination catalyzed by vanadium bromoperoxidase. Inorg Chem 29:5015-5017.

Suzuki T, Suzuki M, Furusaki A, Matsumoto T, Kato A, Imanaka Y, Kurosawa E (1985) Teurilene and thyrsiferyl 23-acetate, *meso* and remarkably cytotoxic compounds from the marine red alga *Laurencia obtusa* (Hudson) lamouroux. Tetrahedron Lett 26:1329-1332.

Suzuki M, Matsuo Y, Takeda S, Suzuki T (1993) Intricatetraol, a halogenated triterpene alcohol from the red alga *Laurencia intricata*. Phytochem 33:651-656.

Suzuki M, Vairappan CS (2005) Halogenated secondary metabolites from Japanese species of the red algal genus *Laurencia* (Rhodomelaceae, Ceramiales). Curr Top Phytochem 7:1-34.

Taylor MT, Fox JM (2015) Biosynthesis of the C15-acetogenin laurepoxide may involve bromine-induced skeletal rearrangement of a Δ4-oxocene precursor. Tetrahedron Lett 56:3560-3563.

Undurraga SF, Press MO, Legendre M, Bujdoso N, Bale J, Wang H, Davis SJ, Verstrepen KJ, Queitsch C (2012) Background-dependent effects of polyglutamine variation in the *Arabidopsis thaliana* gene *ELF3.* Proc Natl Acad Sci 109:19363-19367.

Wang B, Gloer JB, Ji N, Zhao J (2013) Halogenated organic molecules of Rohodomelaceae origin: Chemistry and biology. Chem Rev 113:3632-3685.

Wever R, van der Horst MA (2013) The role of vanadium haloperoxidases in the formation of

volatile brominated compounds and their impact on the environment. Dalton Trans 42:11778-11786.

Wever R, Krenn BE, Renirie R (2018) Marine vanadium-dependent haloperoxidases, their isolation, characterization, and application. Methods Enzymol 605:141-201.

Weyand M, Hecht HJ, Kieß M, Liaud MF, Vilter H, Schomburg D (1999) X-ray structure determination of a vanadium-dependent haloperoxidase from *Ascophyllum nodosum* at 2.0 Å resolution. J Mol Biol 293:595-611.

Wischang D, Hartung J (2011) Parameters for bromination of pyrroles in bromoperoxidase-catalyzed oxidations. Tetrahedron 67:4048-4054.

Zhang Y-A, Yaw N, Snyder SA (2019) General synthetic approach for the *Laurencia* family of natural products empowered by a potentially biomimetic ring expansion. J Am Chem Soc 141:7776−7788.

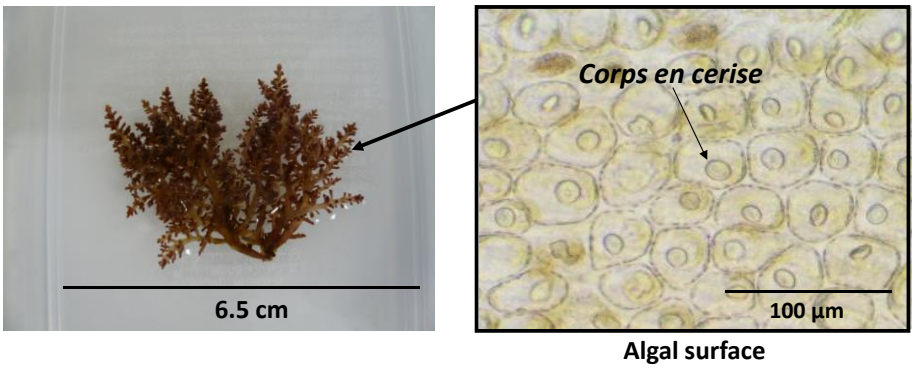

Fig. 1. *Laurencia saitoi* collected at Oshoro Bay (Hokkaido, Japan) in July 2011. The *corps en cerise*, an organelle storing brominated compounds was observed at the surface.

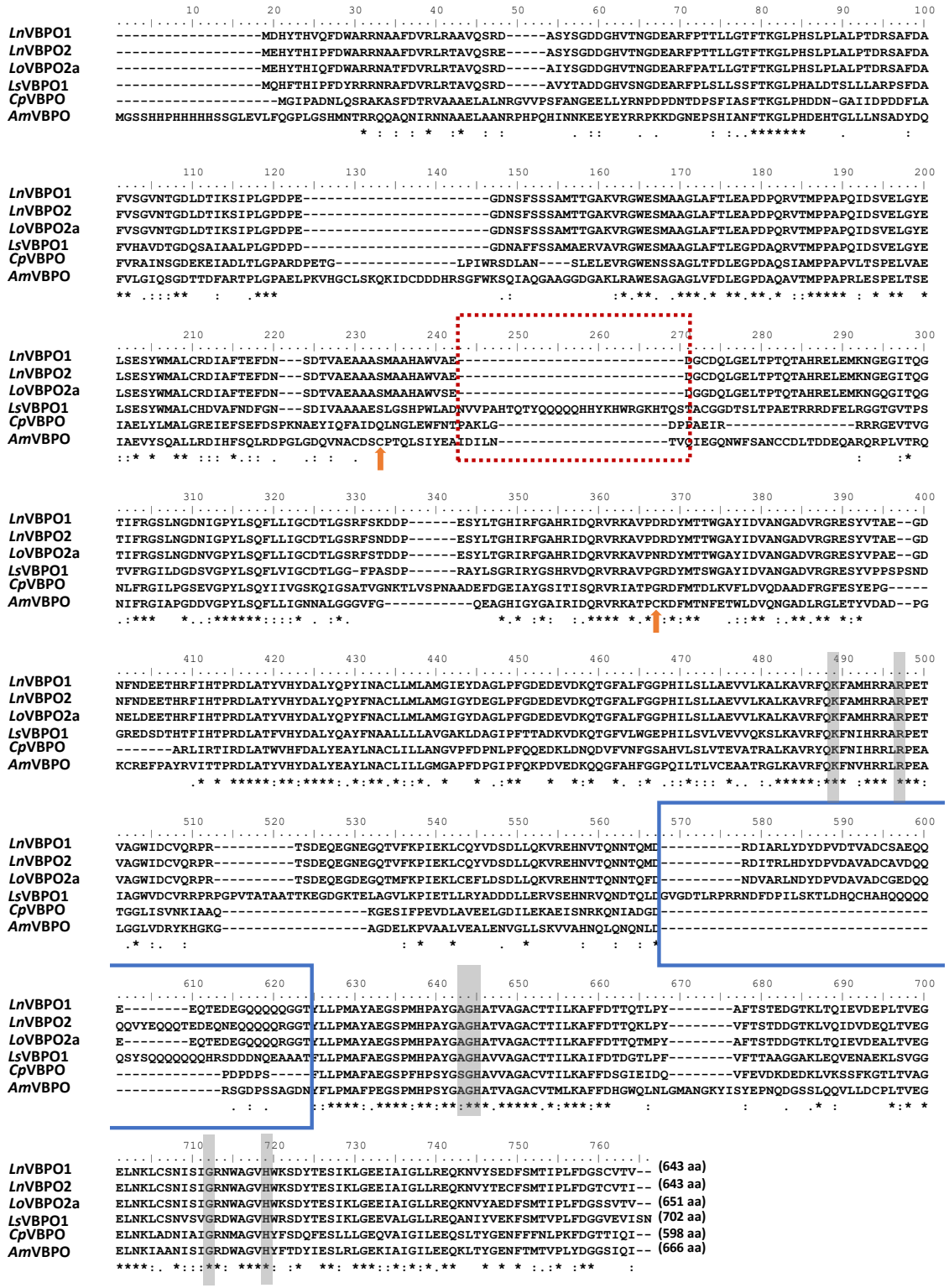

Fig. 2. Amino acid sequence alignment of V-BPOs from *Laurencia saitoi*, *L. nipponica*, *L. okamurae*, *Corallina pilulifera,* and *Acaryochloris marina*. *Ls*VBPO1, *Ln*VBPOs, and *Lo*VBPO2a are V-BPO from *L. saitoi*, *L. nipponica*, and *L. okamurae*, respectively. As the comparisons, the V-BPOs from the red alga *Corallina pilulifera* (1up8_A: *Cp*VBPO) and the cyanobacterium *Acaryochloris marina* (5LPC_A: *Am*VBPO), which have had their X-ray

crystal structures characterized were chosen (Littlechild and Garcia-Rodriguez 2003; Frank et al. 2016). The shadowed residues denote the principal residues responsible for enzymatic activities and vanadate center. The block enclosed with the solid blue line contains a specific insert with Gln repeats in *Laurencia* (Gly512-Thr568). The block enclosed with the dotted red line contains an additional insertion specific to *Ls*VBPO (Asn194-Ser221). The arrows colored in orange show the Cys residues forming *inter*-/*intra*-disulfide bonds in *Am*VBPO. *Ls*VBPO shares 37% and 39% identities to *Cp*VBPO and *Am*VBPO, respectively.

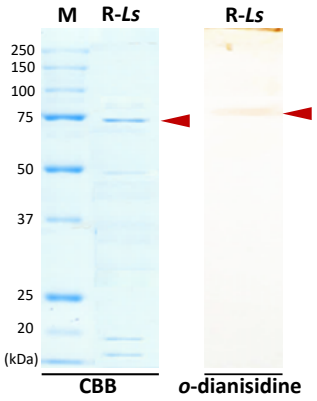

Fig. 3. SDS-PAGE (10%) of partially purified recombinant *Ls*VBPO1 protein.
Lane M contains a 20-250 kDa molecular weight marker. Lanes R-*Ls* are IPTG-induced recombinant proteins of *Ls*VBPO1 (0.8 M KBr fraction after DE52 anion-exchange chromatography). Partially purified *Ls*VBPO1 was verified as a band of approximately 75 kDa on CBB staining (red arrow, 77.0 kDa). Recombinant *Ls*VBPO1 protein was also stained with *o*-dianisidine for in-gel active staining (Carter et al. 2002). The slight difference in the band position between CBB and *o*-dianisidine might be due to differences in staining and washing.

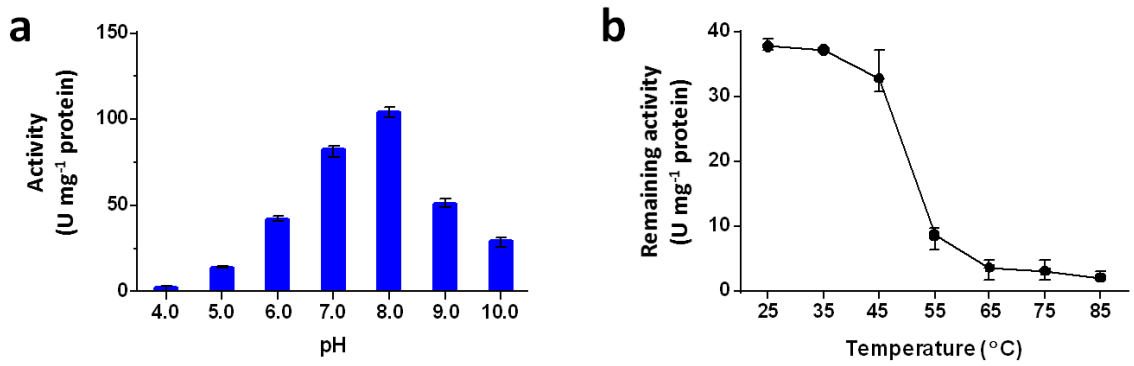

Fig. 4. pH dependency and thermal stability of recombinant *Ls*VBPO1 protein.
a: MCD activity at different pH values; b: thermal stability. After treatment with enzymes at various temperatures (25-85°C) for 20 min, MCD activity was assayed.

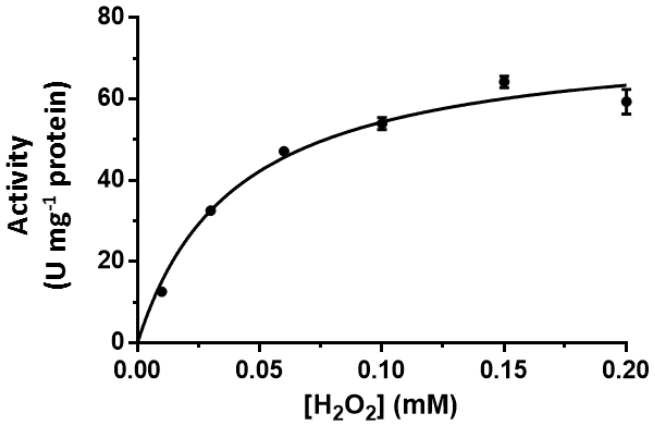

Fig. 5. Steady state kinetics for H_2O_2.

Table 1. Comparison of biochemical behavior of recombinant proteins of *Laurencia* V-BPOs.

	***Ls*VBPO1**	***Ln*VBPO 1**	***Ln*VBPO 2**	***Lo*VBPO2 a**
Molecular weight	77 kDa	71 kDa	71 kDa	71 kDa
Purification degree	**Partially purified**	Single band on SDS-PAGE	Single band on SDS-PAGE	Single band on SDS-PAGE
Bromination activity (U mg^{-1} protein)	**38**	443	434	477
Optimum pH	**8.0**	7.0	7.0	7.0
Inactivated pH	4.0	4.0	4.0	4.0
Activity declined temperature	45-55˚C	45-55˚C	55-65˚C	45-55˚C
K_m for H_2O_2 (mM)	0.04 (± 0.00)	0.026 (± 0.006)	0.025 (± 0.006)	0.014 (± 0.001)
K_m for Br^-	Undetectable	0.53 (± 0.05)	0.35 (± 0.07)	1.38 (± 0.07)
Chlorination activity	Not detected	Not detected	Not detected	Not detected

The biochemical behavior of *Ln*VBPOs and *Lo*VBPO2a referenced from our previous reports (Kaneko et al. 2014 and Ishikawa et al. 2022). Red letters denote unique biochemical behavior in *L. saitoi* (*Ls*VBPO1). K_m values within brackets indicate standard deviations.